Effect of Coinage Metal (Au, Ag & Cu) Loading on CdS Nanorod Composites for Photoreduction of Nitro Organics

A

Thesis submitted

In partial fulfillment of the requirement for the degree of

Master of Science

In

Chemistry

Submitted by

Shubhpreet Kaur

(Reg. No. 301202012)

Under the supervision of

Dr. Bonamali Pal

Head (SCBC), Professor

School of Chemistry and Biochemistry

Thapar University

Patiala- 147 004

Punjab India

July 18, 2014

Certificate

This is to certify that the project entitled "Effect of Coinage Metal (Au, Ag & Cu) Loading on CdSNanorod Composites for Photoreduction of Nitro Organics" being submitted by Ms. Shubhpreet Kaur in partial fulfillment of the requirement for the award of Degree of Masters in Chemistry in the school of Chemistry and Biochemistry, Thapar University, Patiala, is a bonafide work carried out under the supervision of ProfessorBonamali Pal and that no part of this project has been submitted for the award of any other degree.

18/7/14

Professor Bonamali Pal

Head (School of Chemistry and Biochemistry)

Thapar University, Patiala

Dr. S.K.Mohapatra

Senior Professor

Dean, Academic Affairs

Thapar University, Patiala

Candidate's Declaration

I hereby declare that the work being presented in the dissertation entitled "Effect of Coinage Metal (Au, Ag & Cu) Loading on CdSNanorod Composites for Photoreduction of Nitro Organics" in the partial fulfillment of the requirements for the award of the degree of Masters in Chemistry, School of Chemistry and Biochemistry (SCBC), Thapar University, Patiala, is my own work during the period of January to July 2014, under the supervision of Professor Bonamali Pal. I have not submitted the matter embodied in this dissertation for the award of my other degree.

Shubhpreet Kaur

Shubhpreet Kaur

Place: Patiala

Date: 18/07/2014

This is to certify that the above statement made by the candidate is correct and true to the best of our knowledge.

18/7/14

Professor Bonamali Pal
Project Supervisor,
Head (School of Chemistry and Biochemistry)
Thapar University, Patiala

Acknowledgement

I take this opportunity to pay my deep sense of gratitude to my supervisor ProfessorBonamali Pal for his guidance and support in doing my project work.I thank Mr. Rohit Singh, Research Scholar for his guidance and support to me.I also thank the laboratory staff for their timely help.I thank all other faculty members, friends and my beloved parents for their help and motivation.

Shubhpreet Kaur

Shubhpreet Kaur

List of Contents

Abstract

This thesis demonstrates the preparation and characterization of 1 wt % coinage metal loaded CdS nanorod composites (Photodeposited and doped) in argon atmosphere under direct sunlight to study the photoreduction of nitroaromatics (*p*-nitrophenol, *p*-chloronitrobenzene and *p*-dinitrobenzene). The optical properties are characterized by diffused reflectance spectra, photoluminescence, X-ray diffraction and the photoactivity study is done by UV-vis spectroscopy and HPLC. It is found that the coinage metal (Au, Ag & Cu) loaded CdS nanorods showed always better photoactivity than bare CdS nanorods, due to the fact that, metal loading prevents the electron-hole recombination rate of the photogenerated charged carriers and also decreased the band gap. Among metal photodeposited and metal doped CdS-nanorods, metal doped showed better optical and photoactivity because of higher photoexcited charge separation ability, uniform dispersion of metal $^{n+}$ ions, surface structural distortion, imparting extra electrons and uniformly mixing of metal with crystal, which resulted in the ease of charge transfer to reactant species.

1. Introduction

Unique features of nanomaterials such as larger surface to volume ratio, faster charge transport to surface, more surface atoms and controllable morphology etc. distinguish them from their bulk phase [1-4]. In spherical crystals, benefits arising from the higher surface to volume ratio with decreasing the particle size are significantly offset by the increased e^-/h^+ recombination probability at surface trapping sites [3-5]. On the other side, anisotropic nanocrystals (NC), such as nanorods (NR) and nanowires (NW) have attracted widespread attention due to their better quantum confinement effect relative to conventional spherical nanoparticles [5-6] As a result, many beneficial physicochemical properties can be improved in terms of availability of different atomic planes on crystal facets, two-dimensional quantum confinement effect, larger per–particle surface area, high diffusion of charge carriers, length to diameter controlled absorption & emission and higher lifetime of photogenerated charge carriers etc. shapes [7-9].

For an example, cube like morphology of Ag-NP has been found to be nearly 14 times more active for the oxidation of styrene than its plates like shape, and 4 times more active than its spherical shape [10]. Zhou et al. exposed that CeO_2 nanorods [11] having (001) and (110) planes exhibited higher catalytic activity for CO oxidation than do by nanospheres. Considering this, different anisotropy metallic (Cu, Ag, Au and Pt) or semiconducting (TiO_2, ZnS, ZnO, CdS and $BiFeO_3$) nanostructures were broadly studied [12-15] for photovoltaic, photocatalytic hydrogen production and degradation of toxic pollutants etc. But the main challenge in the development of a photocatalyst has been fulfilled by the following conditions;

- Suitable band edge potentials for redox reactions.
- Long term stability during the overall photocatalytic reaction.
- Narrower band gap (E_g < 3 eV) for maximum coverage of light spectrum.

The absorption in the UV light (λ < 380 nm; approximately 3 to 4% of sunlight) and fast recombination of photoexcited charge carriers in wide band gap metal oxides (Eg > 3 eV; TiO_2, WO_3 and ZnO etc.) impair their applications to a greater extent [16,17]. In contrary, metal chalcogenides, especially, cadmium sulfide (CdS), a visible light-driven photocatalyst having band gap ~2.42 eV and suitable negative flat-band potential make it a promising material [18-21] for practical applications. Due to its suitable oxidation potential (+2.0 eV vs NHE), it is usually used for the wastewater treatment and decolourization and mineralization

of dyes. It is also known to be one of the most potential photocatalyst because of their high reduction potential over Nitro group (-0.5 V). The conduction band position [22,23] relative at negative potential (-0.4 eV) offer CdS excellent photocatalytic activities for the photoreduction of H^+ to H_2 and NO_2 to NH_2.

It is well proven that the activity of CdS can be further improved by modifying its surface with metal nanoparticles (NPs). The free electrons can transfer from semiconductor to metal (M) side (if $\phi m > \phi s$) until their Fermi levels are aligned *(Scheme 1)* by generation of a Schottky barrier through M-SC interface [24,25].

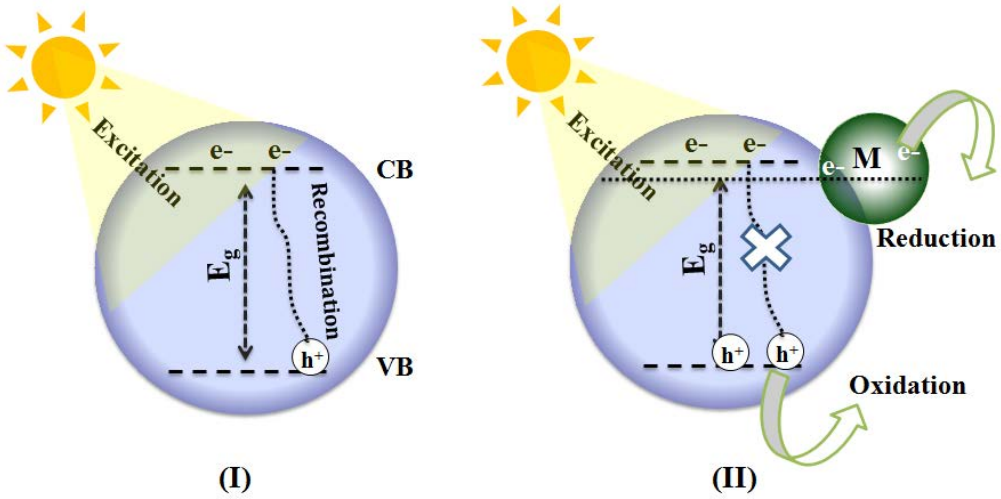

Scheme 1. Illustration of charge separation in bare and metal modified CdS nanocomposites.

Case I: In conventional photocatalysis the photoexcited electron have a probability to come back to the valence band level without reacting with adsorbed species and this process dissipating the energy in the form of light or heat. This recombination is undesirable and leads to an inefficient photocatalyst with poor quantum efficiency.

Case II: Effect of metal loading

Metal loaded on the CdS surface may act as a unique pathway for capture, storage and discharges of photogenerated electrons. Generally, metal in contact with semiconductor accumulate excess charge prior to recombination, thus improving the interface charge-transfer process [26-29]. Choice of metal is done on the basis of their reduction potential, so that the metals which having lower reduction potential than SC are preferred, as more and more electrons get transferred to the metal and further to the reacting species.

2. Literature review

To improve the quantum efficiency and lifetime of photogenerated charge carriers, various metals (Au/CdS, Ag/CdS, Mn/CdS, Fe/CdS, Ni/CdS etc) are deposited on to the CdS surface [27-31]. Among various metals, Au, Ag and Cu considered to be promising candidate [32,33] due to their fascinating resonant behavior after interacting with UV and visible light photons, stability, and size-, shape dependent Fermi level equilibration.

Makori et al. attempted [34,35] to selectively grow the Au nanocrystals (NC) onto the CdS surface to avoid the growth of metal clusters over the entire rod, with less selectivity for the tips. Matchstick, dumbbell and double dumbbell like fascinating morphologies of Au-CdS has been successfully optimized by this group. Au growth on the CdS nanorods by thermal and light induced routes has been also reported for the observed change in photoluminescence. The solution phase synthesis of CdS nanorods and Au nanocrystals of ~2 nm in diameter were grown on the CdS surface in the presence of $NaBH_4$ for improved photocatalytic activity [36].

It is also reported that Platinum loaded CdS powder having a hexagonal crystal structure has been found to be much more efficient as a photocatalyst in hydrogen production than that having a cubic crystal structure [18]. ***Khon et al***. scrutinized the nature of exciton-Plasmon interactions in Au-tipped CdS nanorods and observed that strongly coupled systems promote mixing of electronic states at semiconductor-metal domain interfaces, which causes a significant suppression of both Plasmon and exciton excitations of carriers [37].

Time resolved emission studies of Ag-adenine-templated CdS (Ag/CdS) nanohybrids were investigated in detailed. The observed changes in fluorescence behavior in terms of intensity, lifetime and spectral shift are nicely discussed by considering electronic interaction between Ag and CdS phases [30]. Photo-catalytic H_2 production activity of CdS nanorods was tested and compared with bulk CdS, calcined CdS, noble metal (0.2% Pt) loaded CdS by Janet et al. Surface area, pore volume and band gap were correlated to justify the observed change [22].

The photocatalytic activity and stability of a CdS was successfully improved by metal doping and simultaneous deposition. They have found that enhancement in activity is due to the fast transfer of photogenerated electrons from the conduction band of CdS to Ag nanoparticles on the surface and enhancement in stability is due to doping with Ag, which creates an acceptor energy level near the valence band of CdS prior to recombination [38].

Recently, ***Singh et al.*** have reported the influence of contact area of M-SC junctions developed by different geometrical orientations of Au and CdS nanoparticles. It is

experimented that Au (nanorod) – CdS (nanorod) interface proved to be highest photoactive, owing to the longer relaxation lifetime of photoexcited charge species than conventional metal–semiconductor junctions [39].

3. Rationale of Thesis

Literature review suggests that most of work has been done regarding the synthesis of M-CdS nanocomposites. Up to this date, much effort has been employed to elucidate the growth mechanism, optical, structural, fluorescence emission properties to achieve the best information in CdS and M-CdS nanostructures.

It has been concluded that:

- M/CdS (M = Au, Ag and Cu) nanocomposites are mainly investigated for growth mechanism, interactions, and their photoluminescence properties, but their influence onto the controlled photoredox reactions are rarely noticed.
- Coinage metal nanoparticles were mainly deposited onto spherical nanoparticles of CdS, but very few reports have discussed the effect of deposition or doping on to CdS nanorods for further improvement in their optical and photocatalytic properties.
- The comparative study of coinage metal deposited and doped CdS nanorods has not been considered yet.

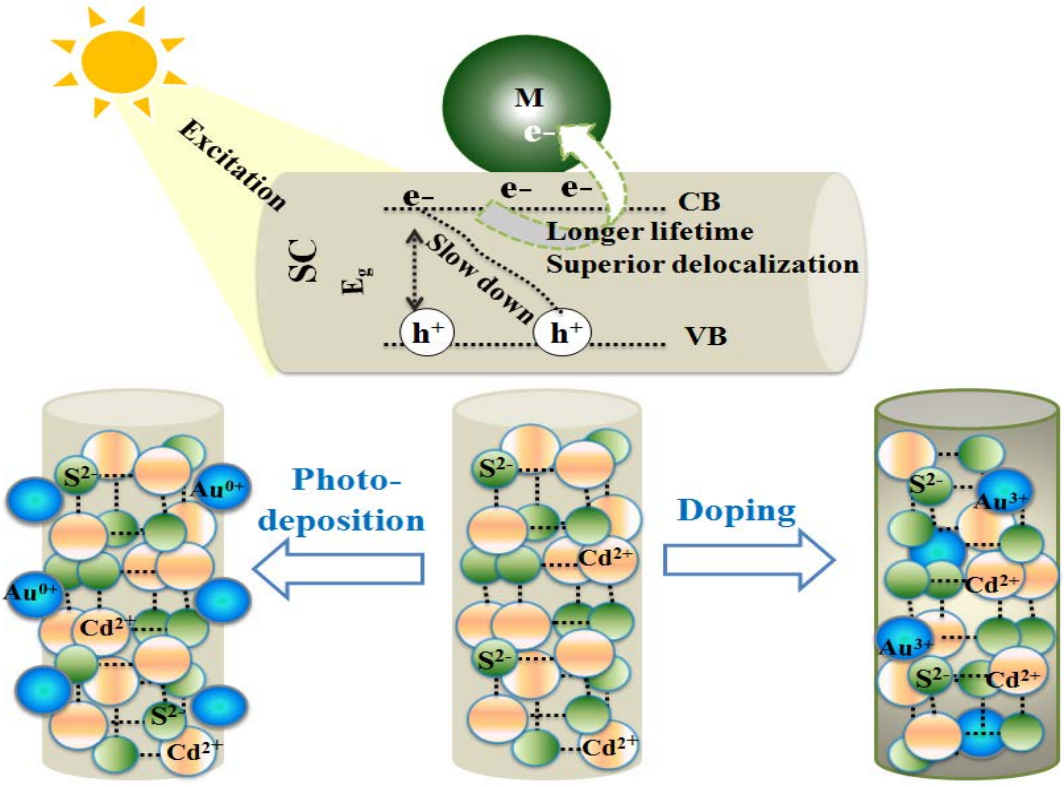

Scheme 2. Graphical representation of charge transfer in M loaded CdS nanorods (above) and below is its structural-morphological difference after photodeposition and doping of techniques.

As shown in scheme 2, the intentional incorporation of M^{n+} (say Au^{3+}) into CdS crystal lattices by replacing some Cd^{2+} ions led to a homogeneous dispersion of Au^{3+}-CdS junctions throughout the crystal, which is believed to result in the better ohmic contact relative to Au^{0} photodeposited CdS composites.

4. Objectives

Keeping in view the above points, the following objectives have been designed

[1] Preparation and characterization of bare and coinage (Au, Ag & Cu) metal loaded CdS-NR composites.

[2] To investigate the comparative optical and photocatalytic activity of M-CdS composites for photoreduction of nitroaromatics (*p*-nitrophenol, *p*-chloronitrobenzene and *p*-dinitrobenzene).

5. Synthesis and Experimental Techniques

5.1. Materials

Cadmium nitrate tetrahydrate ($Cd(NO_3)_2.4H_2O$), ethylenediamine ($H_2NCH_2CH_2NH_2$), thiourea ($SC(NH_2)_2$), hydrogen tetrachloroaurate(III) hydrate ($HAuCl_4.xH_2O$), silver nitrate ($AgNO_3$. xH_2O), copper nitrate ($CuNO_3.4H_2O$), *p*-dinitrobenzene ($C_6H_4N_2O_2$), *p*-phenylenediamine ($C_6H_8N_2O_2$), *p*-nitroaniline ($C_6H_4N_2O_2$), isopropanol (C_6H_8O), *p*-chloronitrobenzene ($C_6H_4ClNO_2$), *p*-chloroaniline (C_6H_6ClN), *p*-nitrophenol ($C_6H_5NO_3$), *p*-aminophenol (C_6H_7NO) were purchased from Loba Chemicals and used without further purification. Deionized water was obtained using an ultra-filtration system (Milli–Q, Millipore) with a measured conductivity 35 mho cm^{-1} at 25 ºC.

5.2. Synthesis of CdS nanorods

CdS nanorods were synthesized by refluxing of cadmium nitrate (0.4 mmol) and thiourea (0.8 mmol) in the presence of 10 ml of ethylenediamine as a solvent at temperature 120 ˚C for 10 h reaction [36]. The product was washed with distilled water and methanol several times to remove the impurities. The final product was dried in an oven at 50 ˚C for half an hour to obtain a yellow CdS powder.

5.3. Photodeposition of Au, Ag and Cu nanoparticles onto CdS nanorods

As prepared 50 mg of CdS powder was suspended in 5 ml of an aqueous solution of isopropanol (50 vol%) in a test tube. An aqueous solution of metal salt ($HAuCl_4.xH_2O$ or $AgNO_3$ or Cu $(NO_3)_2$) was injected into above test tube. Test tube was sealed with a rubber septum and purged under argon (Ar) atmosphere for 15-20 min to remove any traces of oxygen (Fig. 3). Resulting solution was photoirradiated by UV light (125 W Hg arc-10.4 mW/cm^2) under magnetic stirring for 2 h. The metal was reduced by photogenerated electrons on CdS surface. The resultant powder was washed repeatedly with distilled water and ethanol then dried in oven at 80 ºC for 30 min**.**

5.4. Doping of Au, Ag and Cu into CdS nanorods

In a typical procedure, (0.4-*x* mmol) of $Cd(NO_3).4H_2O$ and *x* mmol of $HAuCl_4.xH_2O$ (or Ag and Cu metal) were mixed thoroughly in 10 ml of ethylenediamine prior to the addition of thiourea (0.8 mmol) and refluxed at 120 ˚C for fixed 10 h. The products were obtained by centrifugation, washing with distilled water and ethanol, and then dried at 60 ˚C for 1 h.

5.5. Characterizations

The optical properties were studied by UV–vis absorption (Analytikjena specord–205) spectrophotometer, diffused reflectance spectrophotometer (Avantes, AvaSpec-ULS2048) and spectrofluorimeter (Perkin–Elmer LS55). The bandgap energy of various samples was evaluated by using Tauc relation, which is given by $\alpha h\nu = A(h\nu - Eg)^{1/2}$ where A is a constant, E_g is the bandgap of the material, α is the absorption coefficient of the material, h is the Planck constant and ν is the frequency of light, respectively. The exact value of the bandgap is estimated by extrapolating the straight-line portion of $(\alpha h\nu)^2$ versus E_g to the x-axis. The surface and structural properties were studied on High resolution transmission electron microscope (HRTEM, FEI Technai G2 F20 operated at 200 keV with resolution of 0.2 Å) and X-ray diffractometer (PANalytical X'Pert PRO with Cu-Kα (k = 1.54060 Å). The average crystallite size was calculated by Scherrer equation ($d = 0.9\lambda/\beta \cos\theta$, where λ, β, θ, d are Cu K*α* wavelength (1.540 Å), full with at half-maximum intensity (FWHM) in radians, diffraction angle and crystallite size, respectively).

5.6. Photocatalytic study

The photocatalytic activity was evaluated for the reduction of 5 ml of substrate (5 mM = 25 μmol) under argon atmosphere in a test tube containing 10 mg of M-CdS catalysts under sunlight irradiation (40-50 $mWcm^{-2}$). The reaction samples after filtration with 0.22 μm

cellulose filter were analyzed by UV–vis spectrophotometer, High Performance Liquid Chromatography (HPLC, Agilent 1120 Compact LC) using C-18 column and MeOH:H_2O (70:30) as a mobile phase at 254 nm wavelength with 1 ml min^{-1} of flow rate.

6. Results and Discussion

6.1. Optical study of 1 wt % coinage metal loaded CdS-NRs

The diffuse reflectance spectra of CdS nanorods in comparison to bare sample is shown in Fig. 1. It has been observed that CdS nanorods showed a blue shift (540 to 510 nm) as compared to bulk CdS, which indicate its quantum confinement effect. It is clearly seen in this figure that after photodeposition and doping, the absorption edge of CdS nanorods showed a red shift. This shift in notable but minute in case of photodeposited Ag-CdS (524 nm) sample, but very significant after doping (540 nm) of Ag^+ in CdS nanorods. The change in absorption spectra of CdS nanorods might be due to their surface modifications with 1 wt % coinage metal nanoparticles.

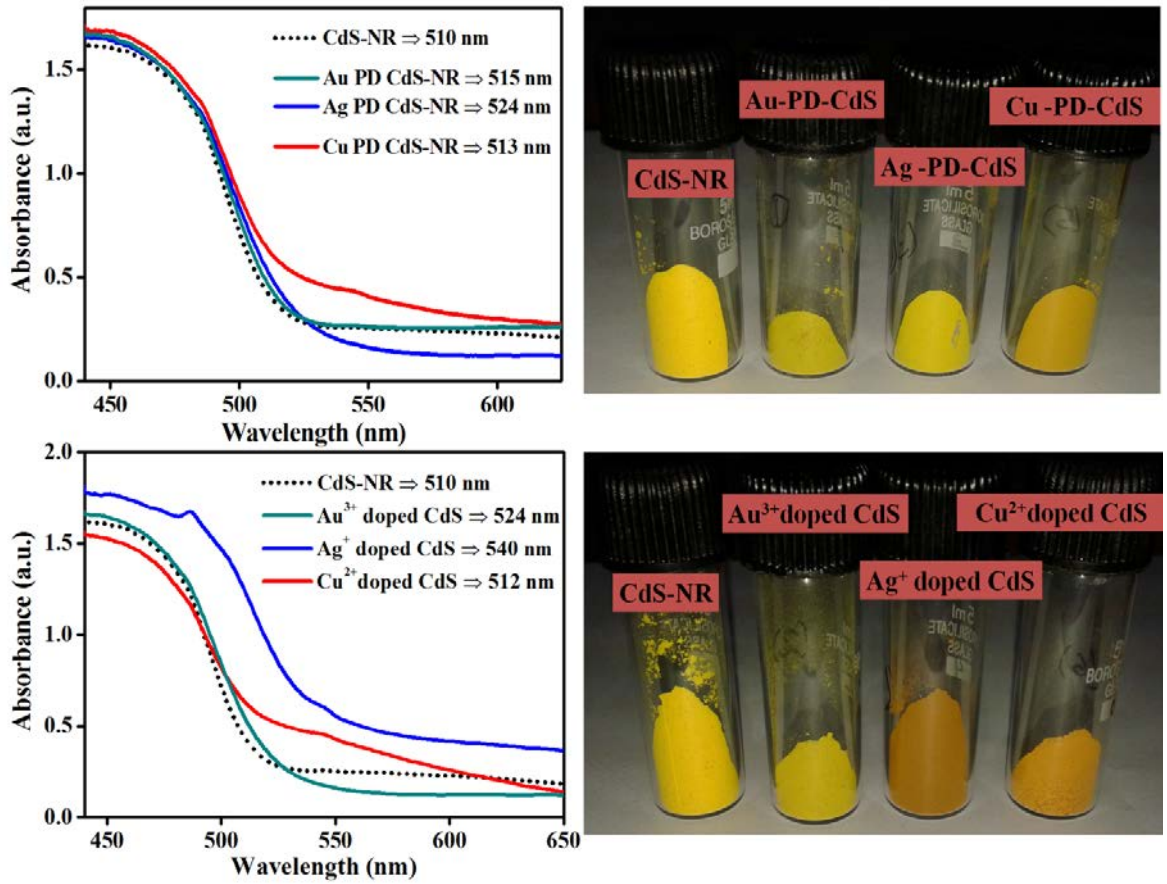

Fig.1. Diffuse reflectance spectra of CdS-NR with 1 wt % coinage metal loaded (photodeposited and doped) CdS-NR.

Interestingly, CdS-NRs shows absorption band around 510 nm but after metal loading, the excitation band of CdS disappeared and show no surface plasmon band due to metal loading, which is very similar with the previous report that indicate these types of nanojunctions facilitates mixing of electronic states at M-SC interfaces which causes suppression of excitation of carriers [37]. The change in absorbance bands of CdS nanorods after surface modifications with coinage metals are further reflected by their variation in colors.

Photoluminescence of bare CdS-NRs and 1 wt % metal loaded CdS-NRs are shown in Fig. 2. In this Fig, bare CdS-NRs shows emission bands at 506 nm due to thermally de-trapped electrons and very weak surface traps at 530 nm due to change in shape and size of the nanorod [40]. PL intensity is mainly decreased by the metal loading on the CdS-NRs because metal loading prevents the electron-hole recombination rates due to rapid delocalization of the photoexcited charge carriers and this delay in the recombination of charged species results to the weak luminescence and due to this high photocatalytic activity is observed due to photogenerated electrons and holes for the oxidation and reduction reactions.

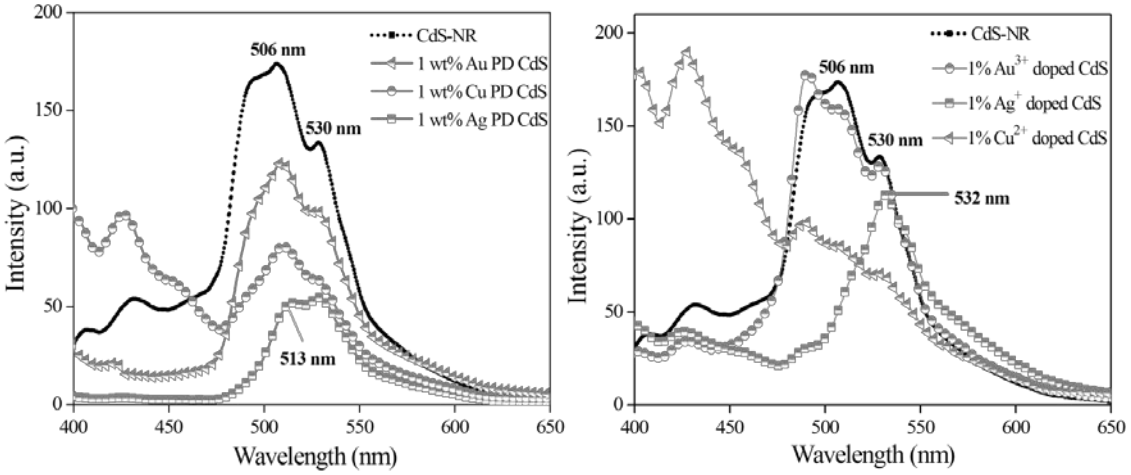

Fig. 2. Photoluminescence of CdS-NR with 1 wt % coinage metal loaded (photodeposited and doped) CdS-NRs.

Notably, when 1 wt % coinage metal loaded on CdS-NRs, the luminescence intensity decreased in case of photodeposited CdS-NRs, however, in case of metal doped CdS-NRs, the luminescence intensity increased as compared to bare CdS-NRs. This is because the recombination centers are blocked that are responsible for the observed luminescence bands and this effect is due to the interaction of doping metals with the recombination sites.

6.2. Structural study

The structural study of the CdS-NRs has been carried out with XRD, which is shown in Fig. 3. All the diffraction peaks are similar and hence possesses hexagonal (wurtzite) crystal structure with lattice parameters (a = b = 4.042 Å, and c = 6.741 Å) which are in good agreement with JCPDS No. 41 – 1049 data card. No any additional peaks and impurities are detected which indicates the high purity of the synthesized products. On coinage metal loading (Au, Ag, Cu photodeposited and doped), the diffraction patterns decreases due to the suppression of electron scattering of CdS-NR by loading of the heavier metals to the CdS surface as the diffraction patterns of coinage metals loaded CdS-NRs almost coincides with the bare CdS-NR and thus indicates that metal particles are well dispersed on the CdS surface.

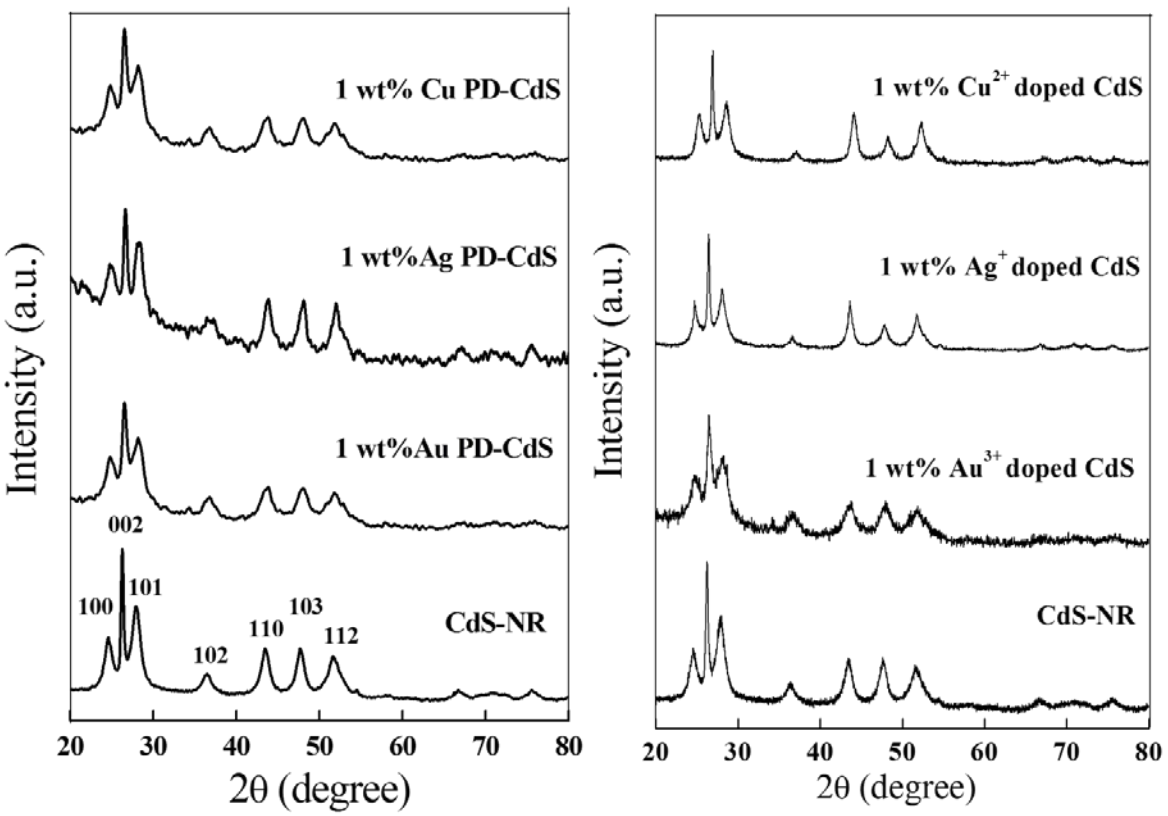

Fig.3. X-ray diffraction patterns of bare CdS-NR with 1 wt % coinage metal loaded CdS-NRs.

6.3. Photoreduction of Nitro-Organic compounds

6.3.1. Photoreduction of p-nitrophenol:

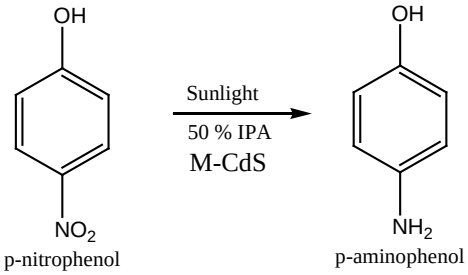

Scheme 3. Illustration showing photoreduction of *p*-nitrophenol to *p*-aminophenol.

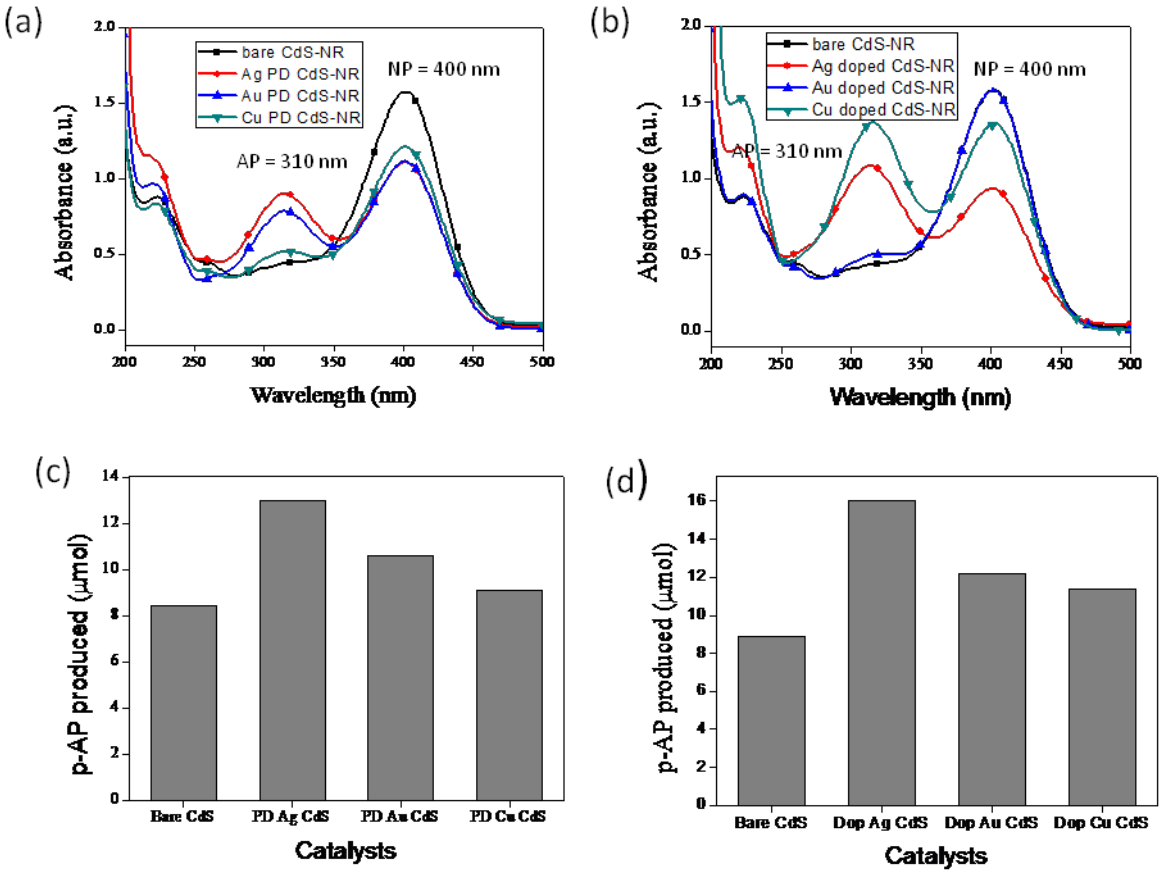

Fig. 4. UV spectra of photoreduction of *p*-nitrophenol (a) with PD CdS-NRs (b) with doped CdS-NRs and the amount of *p*-aminophenol produced (c) with PD CdS-NRs (d) with doped CdS-NRs.

The photoreduction of *p*-nitrophenol was carried out as shown in scheme 3 and it was monitored by UV-Vis spectroscopy as shown in Fig. 4. The comparative study for the photoreduction of *p*-nitrophenol (scheme 3) was done with 1 wt % coinage metal loaded (PD and doped) with bare CdS-NR and was observed that the absorbance of *p*-nitrophenol at 400

nm decreased and a new peak at 310 nm emerged corresponding to *p*-aminophenol due to the photocatalytic effect of CdS. The amount of product formed was found to be more in case of coinage M-PD CdS samples (10-13 μmol) than bare CdS (8 μmol) because of fast transfer of photogenerated charged species to the metal surface which prevents the electron-hole recombination rate. Among the various coinage metals (Au, Ag and Cu), Ag-PD CdS exhibited higher photocatalytic activity for the formation of p-aminophenol (13 μmol) as compared to Au-PD CdS (41 %) and Cu-PD CdS (36 %) nanorods. This is because of fast transfer of photogenerated electrons from the conduction band of CdS to Ag surface as the Fermi level of Ag is closer to the conduction band of CdS. The similar trend was also followed by M-doped CdS samples in which Ag-doped CdS NRs displayed (65 %) yield of *p*-aminophenol in comparison to Au (48 %) and Cu (45 %) doped CdS NRs.

Interestingly, among the M-PD and M-doped CdS samples, M-doped showed better photocatalytic activity, e.g., Ag doped CdS, the amount of *p*-aminophenol formed is higher (65 %) than Ag-PD CdS (52 %) because it enhances the conduction band (CB) of CdS for fast transfer of photogenerated charged species. Moreover, it also increases the energy level difference of CdS CB and M-doped CdS CB so that it increases the excitations. This is due to the better delocalization of the charge carriers which promotes quick electron-hole pair separation and hence reduced the recombination rate and also large surface area of nanorods provides better interfacial contact for charge transfer which prevents electron-hole recombination rate. As compared to PD CdS samples metal doped show better results which is higher in case of Ag doped CdS-NRs because of fast transfer of photogenerated electrons from the conduction band of CdS to Ag nanoparticles and better accumulation of the charge carriers by the Ag doped CdS-NRs will lead to the Fermi level equilibrium which is size dependent with CdS-NRs and hence leads to better charge transfer at the M-CdS interface.

6.3.2. Photoreduction of p-chloronitrobenzene

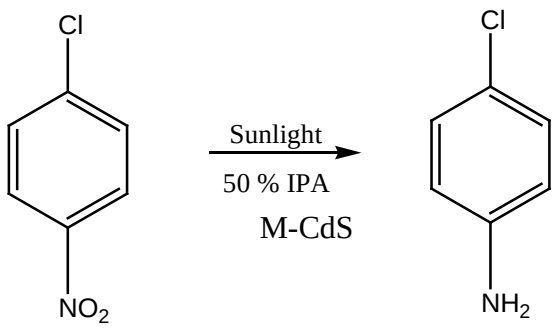

p-chloronitrobenzene p-chloroaniline

Scheme 5. Illustration showing photoreduction of *p*-chloronitrobenzene to *p*-chloroaniline.

Another reaction was carried out for the photoreduction of p-chloronitrobenzene as shown in scheme 5. The aborption band of p-chloronitrobenzene at 280 nm decreased on sunlight irradiation and new peak at 240 nm arose corresponding to its respective amino product. Again 1 wt % coinage metal (Au, Ag & Cu) loaded CdS samples is observed to be highly active than bare CdS-NRs due to the prevention of recombination rate of the photogenerated charged species which also reduces the band gap. The comparative graph for the formation of p-chloroaniline by different catalysts is shown in Fig.5. The M-PD CdS samples showed 9 – 14 μmol concentration of p-chloroaniline than bare CdS-NR (8 μmol} due to better charge transfer which hinders the electron-hole pair recombination rate. Similar trend was followed in case of M-doped Cd Samples but M-doped CdS-NRs was found to show better photocatalytic activity than M-PD CdS-NRs. In case of Ag doped CdS-NR, the amount of product formed is about 64 % than Ag PD CdS-NR (56 %). This is because of the high residence time of photogenerated charged species on the Ag doped CdS surface which slows the electron-hole recombination rate and therefore, accumulation of charge will lead to Fermi level equilibrium for the better charge transfer.

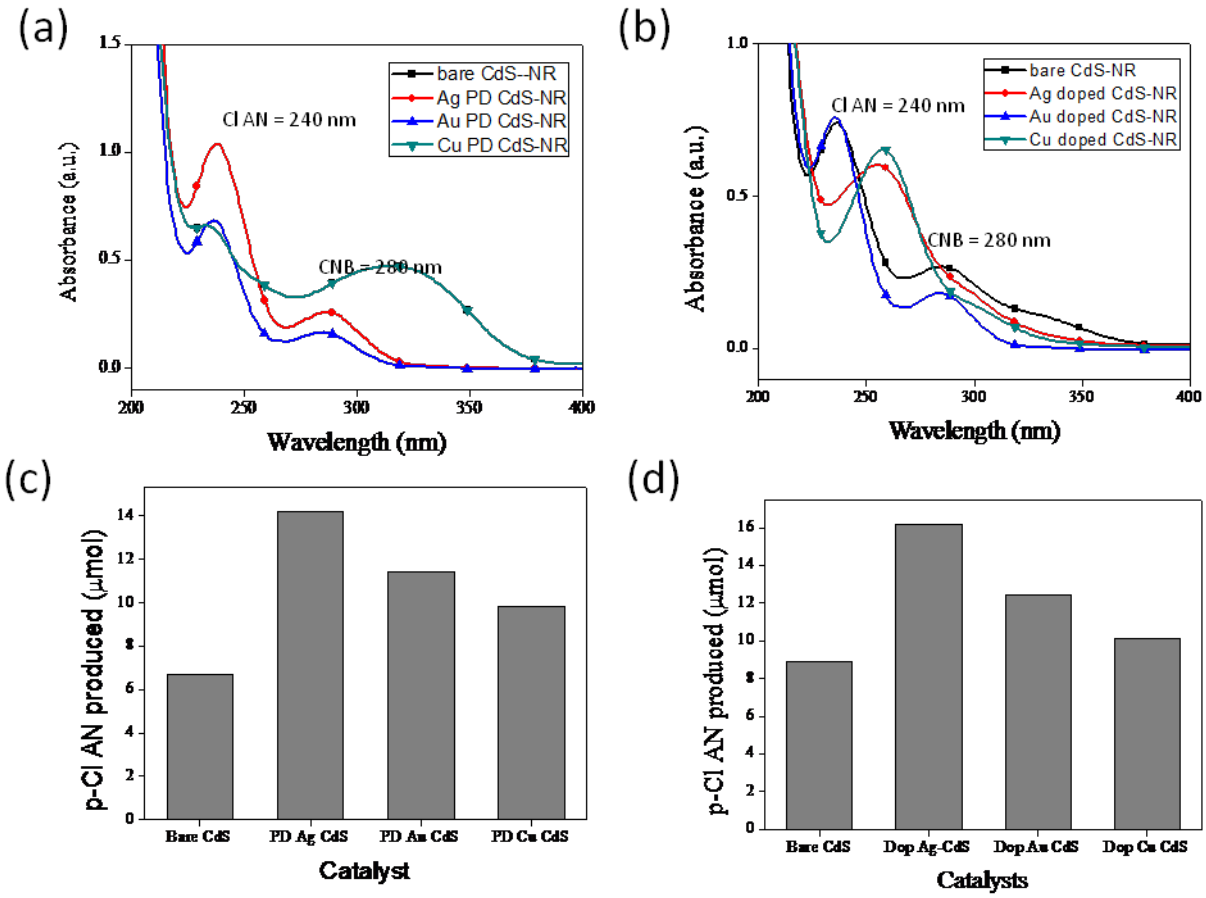

Fig.5. UV spectra of photoreduction of *p*-chloronitrobenzene (a) with PD CdS-NRs (b) with M-doped CdS-NRs and the amount of *p*-chloroaniline produced (a) with M-PD CdS-NRs (b) with M-doped CdS-NRs.

6.3.3. Photoreduction of p-dinitrobenzene:

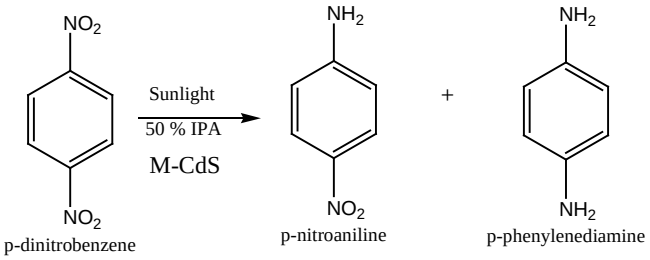

Scheme 6. Illustration showing photoreduction of *p*-dinitrobenzene to *p*-nitroaniline and *p*-phenylenediamine.

Further, the comparative photoreduction of *p*-dinitrobenzene was carried out by M-PD and M-Doped CdS as shown in scheme 6. The reduction process led to the decrease in absorption spectra of dinitrobenzene (240 nm) with the progressive rise of peak at 285 nm corresponding at 285 nm corresponding to phenylenediamine. But the quantitative analysis (HPLC) revealed the formation of another product nitroaniline along with phenylenediamine. The amounts of different products formed by bare and metal loaded CdS is summarized in table 1 below:

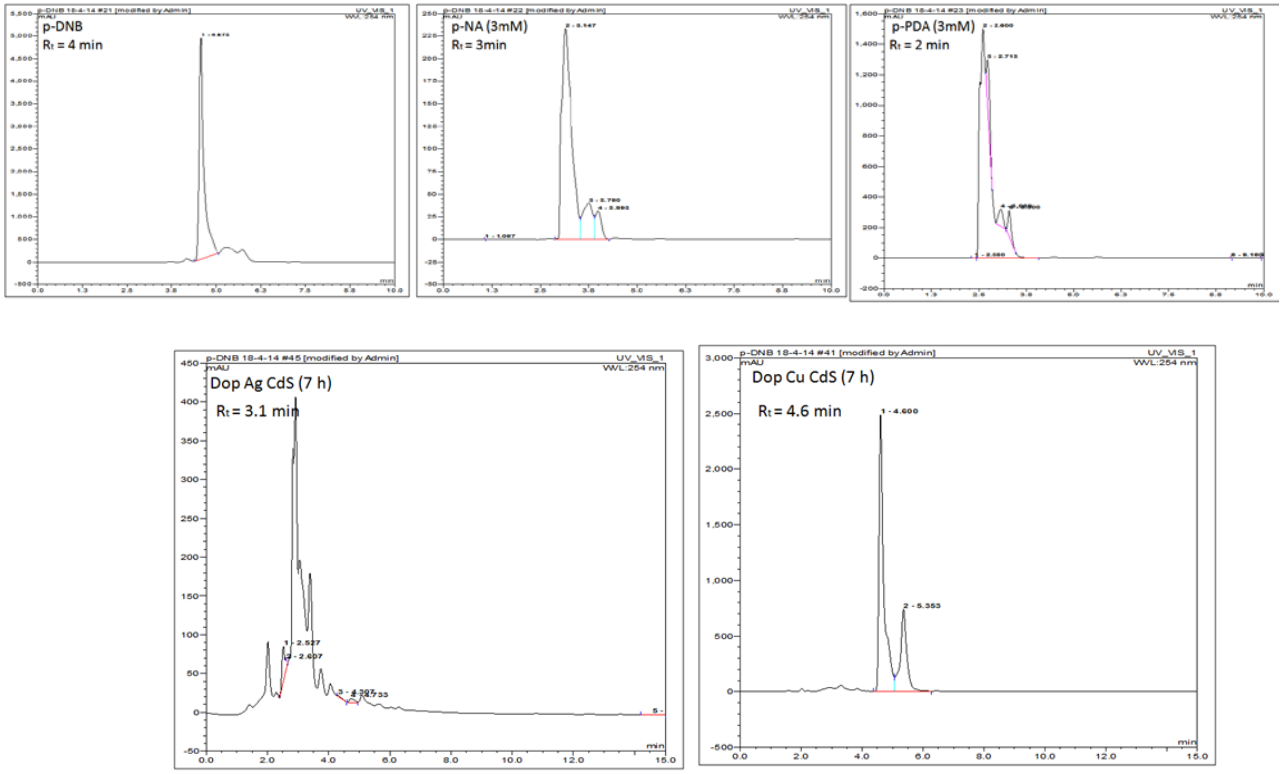

Fig.6. HPLC chromatograms of authentic *p*-dinitrobenzene, *p*-nitroaniline and *p*-phenylenediamine and doped Ag-CdS and doped Cu-CdS.

Table 1. Amount of *p*-dinitrobenzene reduced *(*µmol) and *p*-nitroaniline and *p*-phenylene diamine produced.

Catalyst	***p*-DNB(µmol)**	***p*-NA (µmol)**	***p*-PDA (µmol)**
Bare CdS	14.23	11.6	1.25
Au-PD CdS	14.98	9.7	0.68
Ag-PD CdS	14.67	15	0.98
Cu-PD CdS	13.26	14.98	1.68
Au-Doped CdS	14.88	15	1.68
Ag-Doped CdS	13.03	7.68	2.89
Cu-Doped CdS	7.5	9.35	0.27

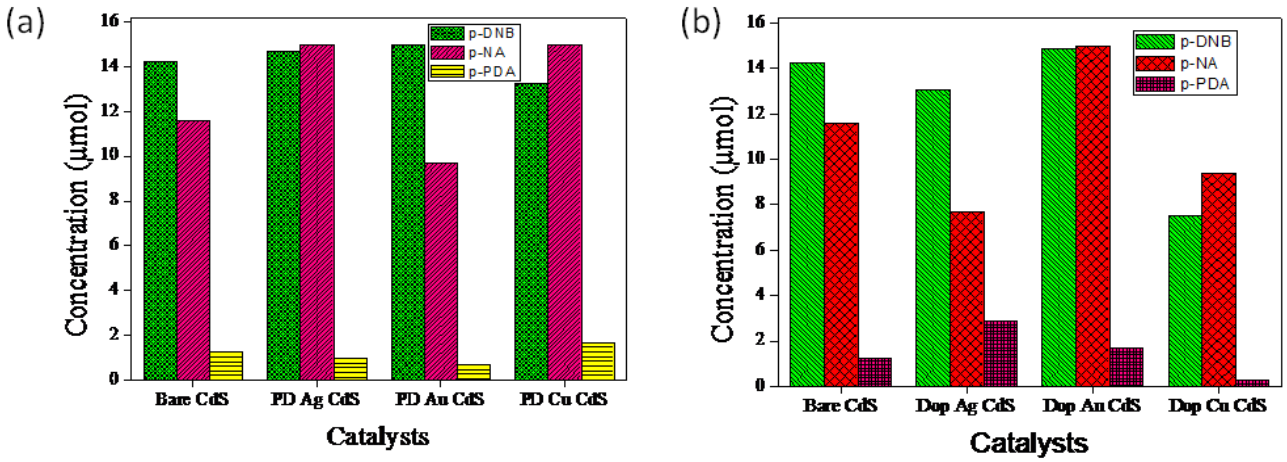

Fig.6. Change in the concentration of *p*-dinitrobenzene and amounts of products formed (a) with M-PD CdS (b) with M-doped CdS.

HPLC chromatogram hows the quantitative amounts of the products formed. As shown in Fig.6. *p*-nitroaniline is produced at Rt = 3.1 minute at apeak height of 400 a.u. after 7 hours in case of Ag doped CdS and the amount of *p*-phenylenediamine is also formed as compared to Cu doped CdS and other metal loaded CdS samples in which amounts of products formed is quite less and very good results are shown in Ag doped CdS because of fast transfer of photogenerated charge species from CdS conduction band to the surface of Ag and it creates the acceptor energy level near the valence band of CdS prior to recombination. Also because of its higher Fermi level equilibrium.

7. Summary and Conclusion

In summary, it was experimented that the 1 wt % coinage metal (Au, Ag & Cu) loaded CdS nanocomposites showed always better photocatalytic activity than bare CdS nanorods for the photoreduction of nitroaromatics (*p*-nitrophenol, *p*-aminophenol and *p*-dinitrobenzene because of the longer relaxation time of the photoexcited charged species at the M-CdS junction. In comparison to photodeposition, doping of coinage metal into CdS nanorods led to remarkable change in their physicochemical properties, which is explained in terms of higher photoexcited charge separation ability, uniform dispersion of metal ions, surface structural distortion, imparting extra electrons and suitable band edge potentials for ease of charge transfer to reactant species for long term activity and stability of lengthy CdS NC under prolong sun light irradiations. Among coinage metal, Ag^{+} doped CdS nanorods composites found to be best photocatalyst due to their higher Fermi level equilibration, which helps in quick charge separation. These observations open up new opportunities to highly improve the efficiency of solar cells with coinage metals modified CdS nanorods.

8. References

[1] S. Linic, P. Christopher, D.B. Ingram, Nat. Mater. 10 (2011) 911.

[2] X. Chen, S. Shen, L. Guo, S.S. Mao, Chem. Rev. 110 (2010) 6503.

[3] A. Mclaren, T.V. Solis, G. Li, S.C. Tsang, J. Am. Chem. Soc. 131 (2009) 12540.

[4] H.J. Yun, H. Lee, J.B. Joo, W. Kim, J. Yi, J. Phys. Chem. C 113 (2009) 3050.

[5] R. Singh, B. Pal, Mater. Res. Bull. 48 (2013) 1403.

[6] Y. Sun, Y. Xia, Science 298 (2002) 2176.

[7] A. Sitt, A. Salant, G. Menagen, U. Banin, Nano Lett. 11 (2011) 2054.

[8] A.E. Saunders, A. Ghezelbash, P. Sood, B.A. Korgel, Langmuir 24 (2008) 9043.

[9] L. Li, C. Nan, Q. Peng, Y. Li, Chem. Eur. J. 18 (2012) 10491.

[10] R. Xu, D. Wang, J. Zhang, Y. Li, Chem.; Asian J. 1 (2006) 888.

[11] K.B. Zhou, X. Wang, X.M. Sun, Q. Peng, Y.D. Li, J. Catal. 229 (2005) 206.

[12] S. Kumar, D. Saini, G.S. Lotey, N.K. Verma, Superlattices Microstruct. 50 (2011) 698.

[13] S. Linic, P. Christopher, D.B. Ingram, Nat. Mater. 10 (2011) 911.

[14] F. Zhang, S.S. Wong, Chem. Mater. 21 (2009) 4541.

[15] G.S. Lotey, N.K. Verma, Chem. Phys. Lett. 574 (2013) 71.

[16] Y. Shiraishi, D. Togawa, D. Tsukamoto, S. Tanaka, T. Hirai, ACS Catal. 2 (2012) 2475.

[17] J. Zhang, Y. Wang, J. Zhang, Z. Lin, F. Huang, J. Yu, ACS Appl. Mater. Interfaces 5 (2013) 1031.

[18] M. Sathish, B. Viswanathan, R.P. Viswanath, Int. J. Hydrogen Energy 31 (2006) 891.

[19] T. Zhai, X. Fang, L. Li, Y. Bando, D. Golberg, Nanoscale 2 (2010) 168.

[20] M. Luo, Y. Liu, J. Hu, H. Liu, J. Li, ACS Appl. Mater. Interfaces 4 (2012) 1813.

[21] J.Y. Hwang, S.A. Lee, Y.H. Lee, S.I. Seok, ACS Appl. Mater. Interfaces 2 (2010) 1343.

[22] C.M. Janet, R.P. Viswanath, Nanotechnology 17 (2006) 5271–5277.

[23] B. Pal, T. Torimoto, K.I. Okazakib, B. Ohtani, Chem. Commun. (2007) 483–485.

[24] Z. Zhang, J.T. Yates, Chem. Rev. 112 (2012) 5520.

[25] N. Zhang, S. Liu, X. Fu, Y.J. Xu, J. Phys. Chem. C 115 (2011) 9136.

[26] A. Wood, M. Giersig, P. Mulvaney, J. Phys. Chem. B 105 (2001) 8810.

[27] V. Subramanian, E.E. Wolf, P.V. Kamat, J. Phys. Chem. B 107 (2003) 7479.

[28] T. Zuo, Z. Sun, Y. Zhao, X. Jiang, X. Gao, J. Am. Chem. Soc. 132 (2010) 6618.

[29] M. Luo, Y. Liu, J. Hu, H. Liu, J. Li, ACS Appl. Mater. Interfaces. 4 (2012) 1813.

[30] A. Kumar, V. Chaudhary, J. Photochem. Photobiol., A 189 (2007) 272.

[31] P.V. Kamat, J. Phys. Chem. B 106 (2002) 7729.

[32] S.D. Borse, S.S. Joshi, Adv. Chem. Lett. 1 (2013) 15.

[33] M.A. El-Sayed, Acc. Chem. Res. 34 (2001) 257.

[34] S.E. Habas, P. Yang, T. Mokari, J. Am. Chem. Soc. 130 (2008) 3294-3295.

[35] T. Mokari, Nano Rev. 2 (2011) 5983.

[36] H. Yang, Metals Mater. Int. 12 (2006) 351.

[37] E. Khon, A. Mereshchenko, A.N. Tarnovsky, K. Acharya, A. Klinkova, N.N. Hewa- Kasakarage, I. Nemitz, M. Zamkov, Nano Lett. 11 (2011) 1792.

[38] S. Huang, Y. Lin, J. Yang, X. Li, J. Zhang, J. Yu, H. Shi, W. Wang, Y. Yu. RSC Adv. 3 (2013) 20782.

[39] R. Singh, B. Pal, J. Mol. Catal. A: Chem. 378 (2013**)** 246.

[40] R. Singh, B. Pal, J. Mol. Catal. A: Chem. 371 (2013) 77.